Simulation and Performance Indices Analysis of Solar Assist Plug-in Electric Tractor

Shawki A. Abouel-Seoud[1], Ahmed Samir El-Adros[1,*],Sameh M. Metwalley[1], Mohamed Watany[1]

Automotive Engineering Department, Helwan University, Cairo, Egypt
Corresponding Author: Ahmed Samir El-Adros

ABSTRACT: *Environmental problems resulting from fuel combustion as a result of its use in internal combustion engines, especially diesel for tractors, as well as the shortage of fossil fuel stocks over time, it is vital to think for an alternative energy source. The adoption of an electric tractor is one such solution. Especially using solar energy as a source of renewable energy to assist in charging battery. In this study, the simulation model of a solar assist electric tractor is created using equations with MATLAB/Simulink. The energy consumption and battery SOC are determined at different tractor's conditions. The simulation of the PV module considered the temperature and sunlight insolation effect. The results of the PV model are validated with I-V and P-V curves of an international published paper. The effect of parameters on tractor performance of energy consumption and battery SOC is examined. The influence of the PV array on battery SOC is presented at different tractor's conditions.*

KEYWORDS: *Electric Tractor, Photovoltaic (PV) cell, Solar Assist Plug-in Tractor, Simulation module, MATLAB/Simulink.*

I. INTRODUCTION

Energy is one of the most important needs of human life on earth [1]. World energy consumption is rising quite rapidly but even worse the reserves' global fossil fuels are running out [2]. One of the biggest challenges in meeting the global demand for energy, which is expected to increase by up to 44% by 2030 [3].

Fig. 1 illustrates the pronounced disparities after the year 2020 between the demand for fuel and world oil production [4].
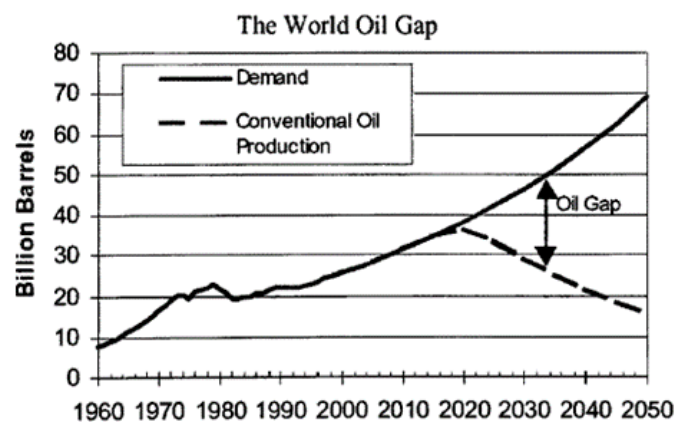

Figure.1. World oil demand by 2050.

Conventional vehicles use petroleum-derived fuels for their internal combustion engine [5]. The combustion of fossil fuel has been associated with several serious global and local environmental issues alongside security concerns and supply longevity [6]. Fossil fuel combustion produces carbon dioxide and greenhouse gases (GHG), thereby increasing their concentration in the atmosphere, causing global warming [6–8]. The average surface temperature of the earth has risen by almost 0.74° C over the previous century. By the end of the 21st century, temperatures are predicted to increase by an additional 3.4° C if we continue to produce carbon without regulation. Climate change of this scale is expected to have significant consequences for Earth's survival. The electricity sector is the key source of overall global CO_2 emissions, accounting for about 40% worldwide, followed by transport, manufacturing, and other industries, as shown in Fig. 2 [7].
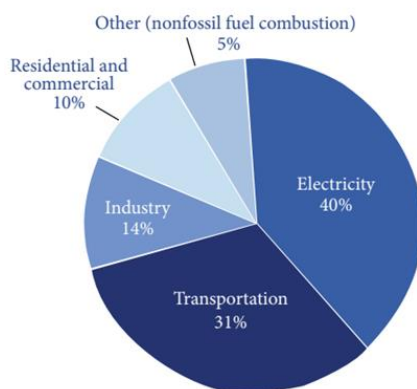

Figure.2. Sources of CO2 emissions by sector

We rely on fossil fuels to fulfill our need for electricity generation, running automobiles, etc [9]. The agricultural tractor is among the most fuel consumers; as a result, the tractor has become a strong focus for electrification research [10]. However, caution should be taken concerning the primary energy source, as emissions from petrol/diesel engines may be counterbalanced by emissions from power stations [11]. All scientists have accepted that solar energy is among the best options for energy supply in many parts of the world [2]. Fig. 3 shows that Egypt is among the top three countries among the Mediterranean countries in solar radiation [6]. Egypt belongs to the global sunbelt with the highest capability for solar-energy projects [11,12].
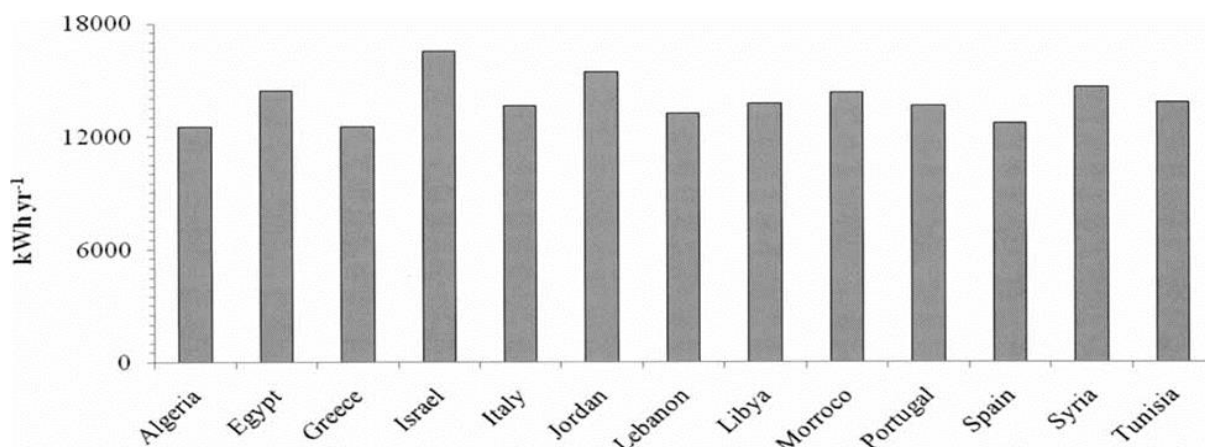

Figure.3. Global solar radiation experienced in Mediterranean countries

Replacing agricultural tractors formerly powered by internal combustion engines with electrical tractors and, preferably, such electrical tractors powered by rechargeable batteries that combine with solar cells have the potential to minimize or eliminate the negative impacts of oil dependence. Specifically, the cost of running a solar electrical tractor should not be impacted by oil depletion. Solar electric tractors do not rely on the combustion of liquid fuels so that agricultural land can remain in food production. However, solar-powered tractors are Zero-emission vehicles such that their use does not produce greenhouse gasses that cause climate change [13].

The Electric Experimental Tractor was tested by Turrel (1969), which was submitted by the Farm Electrification Council and Lead Industries Association in 1969. He identified the EXT as a four-wheeled tractor, equal in capability to a twelve-horsepower gasoline engine unit. The electric tractors (EPT) were more economical to work in terms of energy cost than the petroleum-powered tractor (PPT) for all the operations considered. The EPT saved considerable energy for all field operations because the efficiency energy converter of the electric motor is higher than of its internal combustion engine [14].

A customized drive system for 9 KW family farming electric tractor is studied in [15] using two three-phase induction motors, two independent inverters, and a lead-acid battery bank. Energy consumption is reduced from 29.92 to 16.24 Wh, which reflects a saving of 46 % when the wheel slip control is implemented. Although the power of the electric motor (9 kW) is lower than that of the combustion diesel engine (10.3 kW), the electric tractor's recorded traction force of 4768 N greatly exceeds the traction force of 2365 N produced by the ICE tractor.

Various battery technologies available for use in solar assist plug-in hybrid electric tractors are proposed in [16]. A PV "on board" in a tractor is capable of producing about 4kWh per day, while the transient power of an electric tractor with two 10.5 kW synchronized DC series motors Could reach nearly 60 kW in a few seconds, but the continuous rated power is less than 21 kW. It is therefore important to consider an electric hybrid tractor, with battery and PV, in which the battery stores the excess energy generated by the panel during the day and uses it during the night or in days with low levels of solar radiation.

To allocate parallels brunch to the automotive industry to improve the search for vehicles powered by renewable energy sources, several tractor patents, as required by DOWNING JUNIOR (1978), CHRISTIANSON et al. (1987), ORSOLINI (1995), GINGERICH (1998) and EDMOND (2006), confirmed the concern regarding the design of renewable-energy agricultural machinery. Table 1 shows some of the details of those patents [17].

Patent	Summary	Traction system
CHRISTIANSON et al. (1987)	Tractor for simple jobs. Hydraulic connection steering wheel.	1 engine DC 50 HP for 4-wheel traction; from 930 - 2750 RPM
DOWNING JUNIOR (1978)	Tractor for grain harvest. It features an internal structure (chassis), local service that takes the grain harvested from the front to the back, where there is a blower that sends the grain to a storage location.	4 induction motors, one for each wheel;
EDMOND (2006)	Vehicle coupled to lawn mower or snow blowers. Controller of motors rotation.	1 DC motor for traction on the front wheels
GINGERICH (1998)	Vehicle for cargo transport. Controller of motors rotation.	2 DC motors for traction on the front wheels
ORSOLINI (1995)	The front end of a vehicle for transport.	2 motors for traction on the wheels (1 single axis)

Table.1. Electrical Tractor Patent Details [17].

According to a simulation of an autonomous battery-electric tractor submitted in [18]. Theoretically, it is possible to replace a traditional tractor (160kW) with two autonomous battery-powered machines (36kW motor, 113 kWh battery) with lower costs of 15 percent. Energy consumption will be reduced by 58 percent and greenhouse gas emissions by 92 percent compared to diesel When energy consumption and greenhouse gas emissions from the production of batteries were included.

Design theory, Performance Analysis, and calculation method of the electric tractor were put forward and main component parameters such as motor drive, power battery, and transmission are obtained by Xiaofei Zhang in his paper [19]. MATLAB calculations were performed and the analysis showed that the plow's continuous operating time is up to 6.7 h with a driving speed of 5 km/h.

This paper [20] presented the design and development of a tractor powered by an electric motor for mild plowing operation with a 3kw BLDC motor maintaining a constant operation of 2 hours using Lead-Acid traction batteries. An electric tractor Matlab Simulink model is built, where the output defined the operating zone of the motor, vehicle performance, and battery performance.

The performance of PV system [power output, (Pout), and conversion efficiency, (ηPV)] to operate a developed standalone an electric solar tractor under two tilt angles of PV panel (0 and 30º) is studied in [21]. The results obtained indicated that, for 0 and 30 º tilt angles, the daily average (Pout) of PV is about 1,95 and 2,15 kWh respectively, While the daily average of ηPV is about 13.2 and 13.3 % for 0 and 30º tilt angles, respectively.

SAPHT (Solar Assist Plug-in Hybrid Electric Tractor) was designed, built, and evaluated for light-duty applications in a farm in [22], where approximately 18 percent of SAPHT's daily energy consumption is supplied by an onboard photovoltaic (PV) array and the remaining is supplied via an electricity grid. using the battery pack, a two-ton weighted trailer could be pulled for 2 hours on asphalt at a speed of 25 km/h, for 2.5 h on a sand road at 18 km/h, and 3 h on a field at 9 km/h. The use of batteries with higher energy densities at the same weight would give more operating hours.

From the literature review, it was clear that there was a lack of scientific papers interested in simulating the solar assist plug-in electric tractor. It is important to provide a good model of the car to be able to predict the energy consumption of electric vehicles [23]. Therefore, in this study, a solar assist plug-in electric tractor will be simulated using the Matlab-Simulink program. This model can be used to evaluate the performance of the tractor and solar cells, where energy consumption and battery state of charge (SOC) can be obtained under various operating conditions.

As the first part of the paper will be simulated model for an electric tractor, then a simulation of a validated solar cell model will be done in the second part, and then the electric tractor and solar panel array will be combined into one model in the third part to get results.

II. METHODOLOGY

POWER REQUIRED FROM THE MOTOR

The basic forces acting on the vehicle's movement can be examined in two groups as the forces of resistance affecting the vehicle against the direction of motion (rolling resistance, slope resistance, aerodynamic resistance, inertial resistance, and drawbar force for the tractor) and the driving forces that the motor produces for transmission to the wheels. All these resistances must be overcome by the force produced from the motor to drive the vehicle in the forward direction [24].
Aerodynamic resistance can be neglected as the low speed of the tractor operating, it seems to be insignificant [22]. Due to the insignificance of acceleration for an electric tractor, inertial resistance can be neglected due to the low acceleration value needed.

$Ft = Fst + Fr + Df$ (1)
$Fst = m * g * \sin\theta$ (2)
$Fr = m * g * \cos\theta * Crr$ (3)

Df: is the drawbar force in newton, can be used for towing a trailer or agriculture works like plowing. Assume Df with a maximum 2500 N [20,25].
Fst: is the gradient force, most hills have a gradient of less than 20 % [26]. The tractor is designed to climb a slope of 20 % with a maximum speed of 25 km/hr. where θ = 11.3∘ in degree. Fr: is the rolling resistance force. Assuming the total mass of thesolar assist electric tractor (m) with 2000 kg and rolling resistance coefficient (Crr) with 0.16 [22].
Considering a safety factor of 1.5.
$Fta = 1.5 * Ft$ (4)

The electrical propulsion motor's power requirement is determined by the maximum speed, maximum gradient, maximum drawbar force, and the worst coefficient of rolling resistance of the road surface that the tractor may face [26].

The maximum power required from the motor (pmax) is the power required on the wheels divided by transmission efficiency and motor efficiency [20].

$$\mathbf{P_{max}} = \frac{F_{ta} * V_{max}}{\text{differential efficiency} * \text{motor efficiency}} \ (5)$$

Assuming differential efficiency: 0.90.
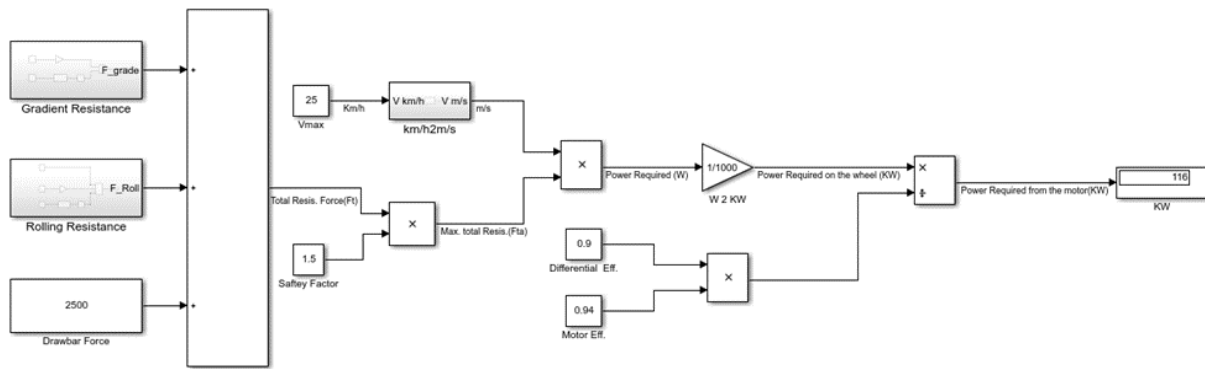Motor efficiency: 0.94 [27].

Figure.4. Maximum Required Power from the motor

The maximum required power from the motor is calculated using Matlab-Simulink with 116 KW according to the assumptions mentioned as shown in Fig. 4 after surveying for a suitable electric motor for this case, the permanent magnet synchronous motor sumo MD HV1500 3p is selected with a maximum peak power of 162 KW and continuous power of 100 KW and its inverter of HV1500-3p [27].

WHEEL TORQUE REQUIRED

Wheel torque required (T) can be calculated using equation 6 as shown in Fig. 5.
$$T = Ft \times rw \qquad (6)$$
where rw: dynamic radius of the wheel, assuming rw= 0.42 m.
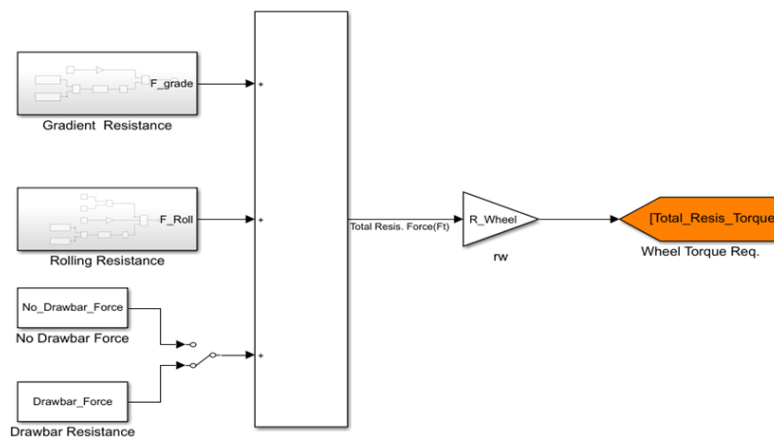
Figure. 5. Wheel Torque Required

TORQUE – RPM CURVE OF THE ELECTRIC MOTOR

The electric motor torque – rpm curve is used to get the maximum torque from the electric motor at a specific rpm, as the electric motor must rotate at rpm that achieves the required vehicle speed. Fig. 6 represents the torque – rpm curve of the selected motor in this study from the motor manufacturer's website [28], where it used to get Fig. 7 by Simulink.
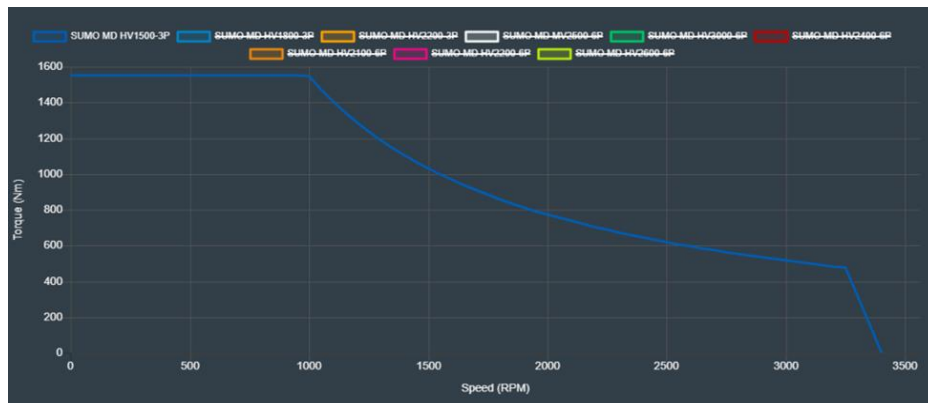
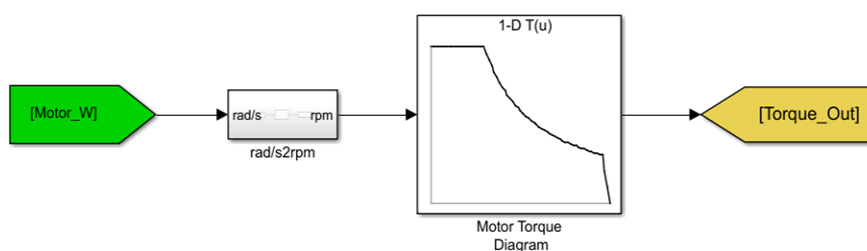**Figure. 6. Torque – RPM Curve of the selected motor**

Figure. 7. Torque – RPM Curve by Simulink

PID CONTROLLER

The PID controller is used in this model to compare the reference speed (drive cycle) and the actual speed. A simple drive cycle is used in this study with a maximum speed of 15 km/hr, where speed up, constant speed, and speed down is used for 900 sec as shown in Fig. 8.
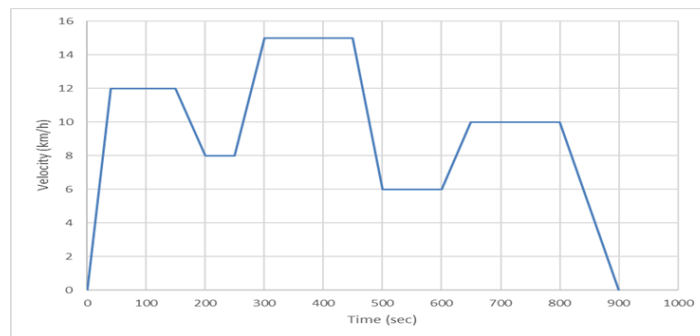

Figure. 8. Simple drive cycle used

The output of the controller is a percentage to be multiplied by the torque output from the motor at the selected motor speed as shown in Fig. 9.
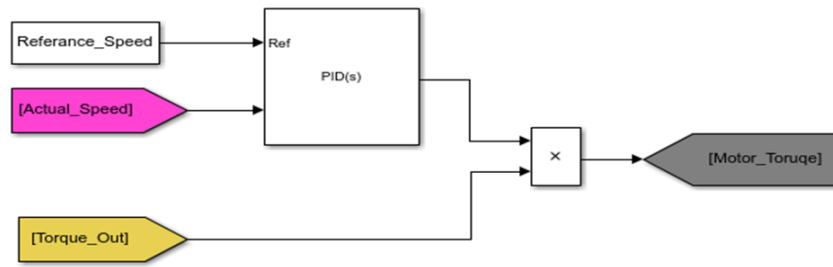
Figure. 9. PID Controller

ELECTRIC MOTOR'S ANGULAR SPEED

$$\frac{dw}{dt} = \frac{Mnet}{J\,total} \qquad (7)$$

Equation 7 represents the relationship between angular acceleration, torque, and moment of inertia; thus, the angular velocity of the electric motor can be calculated by equation 8.

$$Wmotor = \int \frac{(Mmotor * \eta motor) - \left(\frac{Mres}{idiff} * \eta diff\right)}{J\,total} \, dt \qquad (8)$$

Net torque is achieved by subtracting the resistance torque from the electric motor torque, then the actual vehicle speed can be calculated as shown in Fig. 10.
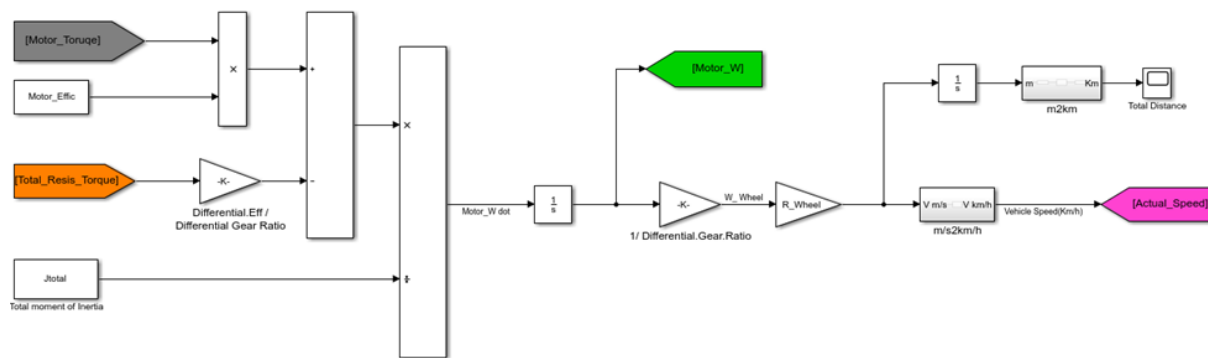
Figure. 10. Angular speed of the Electric Motor and the Actual Speed of the Tractor

Where idiff: Total reduction ratio, assuming idiff = 3.
Jtotal: Total moment of inertia for motor's rotor, assuming Jtotal = 0.3 kg m2.

ENERGY CONSUMPTION AND BATTERY SOC%

Electric energy consumed from the battery can be determined depending on the required motor torque, the angular velocity of the electric vehicle, electric motor efficiency, inverter efficiency as equation 9 state according to the drive cycle time.

$$E = \int_0^{900} \frac{Motor-Torque * Motor-W}{Motor\,Eff.} * Inverter\,Eff. \qquad (9)$$

Due to the lack of accessories (lights, air conditioning, etc.) in this tractor, the corresponding power was not considered.

As there is a source of electric energy storage represented in battery capacity of lithium-ion type which assumed with 25 kw.h.

The battery SOC % can be calculated by subtracting the electric energy consumption (Cused) from the battery capacity (Cmax) then divided by the battery capacity (Cmax) as shown in equation 10 [15]. Since the

photovoltaic array helps in charging the battery thus SOC increasing, the energy from the PV array can be added with a positive signal in the numerator to get the battery SOC with the PV array as shown in Fig. 11.
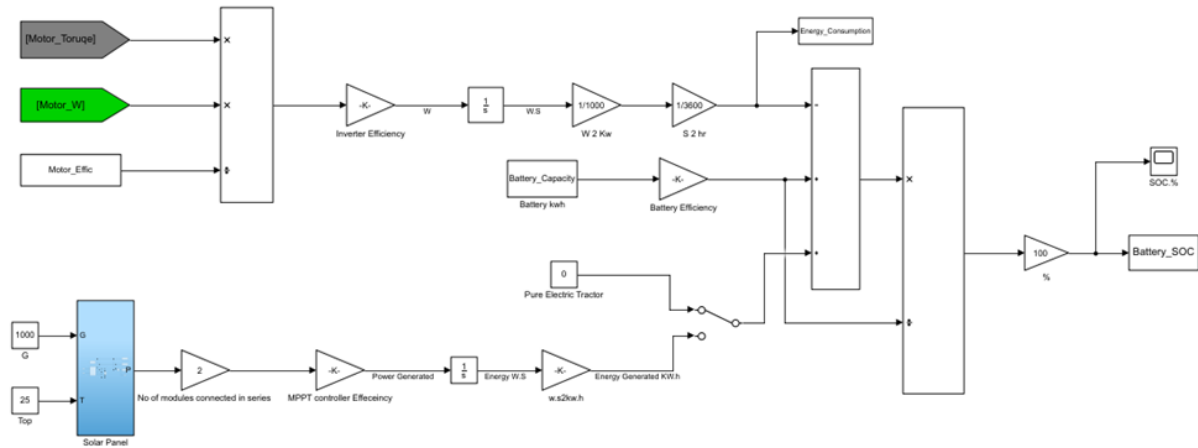
$$SOC\ (\%) = \frac{C_{max} - C_{used}}{C_{used}} \qquad\qquad (10)$$

Figure. 11. Energy consumption and battery SOC (%) of the solar-Assist tractor

SIMULATION MODEL OF THE PHOTOVOLTAIC SYSTEM

The equivalent circuit of photovoltaic single diode cell is shown in Fig. 12, which consists of photocurrent source (Iph) depends on the solar radiation (G) and operating temperature of the cell, diode (D), shunt resistor (Rsh), and series resistor (Rs).
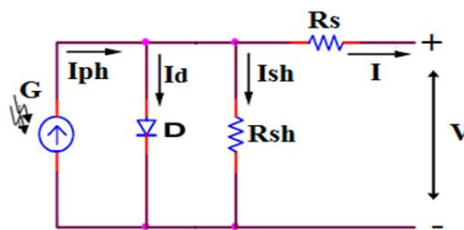

Figure. 12. equivalent circuit of photovoltaic single diode cell

The mathematical equations of the PV cell are required to simulate the equivalent circuit of the photovoltaic cell on MATLAB-Simulink, these equations consider in: -

$$I_{ph} = \frac{G}{G_{ref}}\left[I_{sc} + K_I\left(T_{op} - T_{ref}\right)\right] \qquad\qquad (11)$$

The photocurrent source (Iph) depends on the insolation (G), the short circuit current of the PV cell (Isc), and the operating temperature of the cell (Top).

The Gref and Tref are solar radiation and temperate at Standard Test Conditions (STC) respectively, where Gref = 1000 W/m^2 and Tref = 25°C. KI is the current temperature coefficient. Equation 11 can be simulated using Matlab-Simulink as shown in Fig. 13.
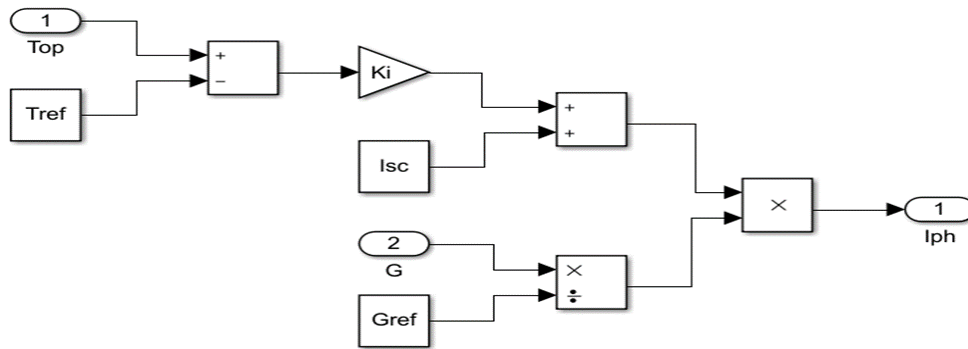
Figure. 13. photocurrent source (Iph)

As shown in Fig. 12, the current I can be concluded as:-

$$I = I_{ph} - I_d - I_{sh} \qquad (12)$$

Where Id is the diode current, and Ish is the current through the shunt resistor (Rsh).

$$I_d = I_{sat}[exp\,(\frac{V + I.R_S}{n.V_t.N_s})] - 1] \qquad (13)$$

Isat is the reverse saturation current of the diode. V is the terminal voltage of the PV cell. n is the ideality factor of the diode, It depends on PV cell technology and it can be chosen from Table 2. Vt is known as thermal voltage because of its exclusive temperature dependence. (Vt = K.T / q). K is Boltzmann constant 1.38 *10-23 J/K, and q is the charge of an electron (q = 1.6 * 10 -19 C). Ns: is the number of cells connected in series for a PV module, where the output of one cell is low around 0.8V [29–32].

Technology	Ideality factor
Si-mono	1.2
Si-poly	1.3
a-Si-H	1.8
a-Si-H tandem	3.3
a-Si-H triple	5
cdTe	1.5
CTs	1.5
AsGa	1.3

Table. 2. ideality factor of the diode (n)

Equations 12 and 13 can be presented using Matlab-Simulink as shown in Fig. 14.
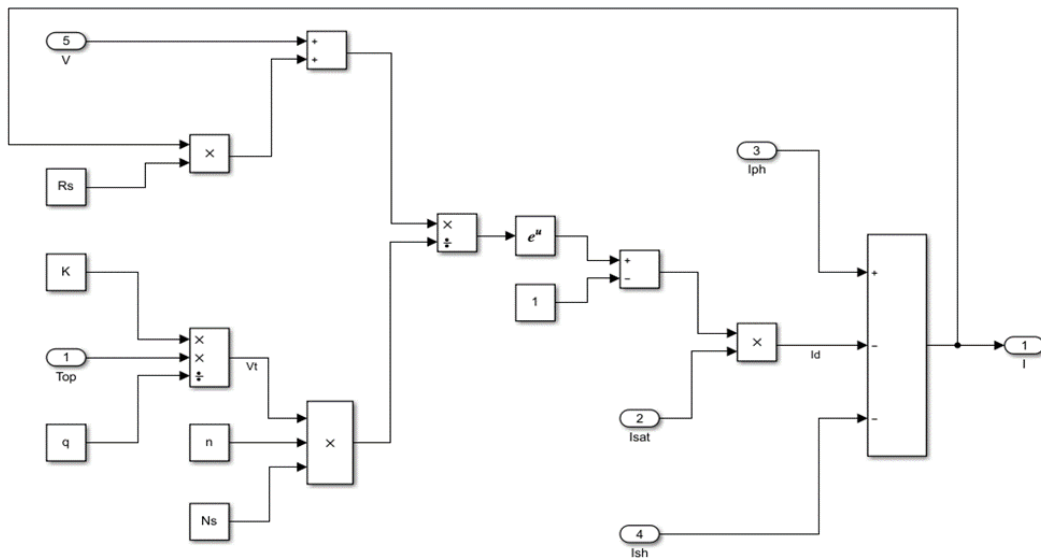
Figure. 14. Output current of the PV module (I)

$$I_{sh=} \frac{V + I.R_S}{R_{sh}} \qquad (14)$$

$$I_{sat} = I_{RS} \left(\frac{T}{T_{ref}}\right)^3 exp\left[\frac{q.E_g}{n.K}\left(\frac{1}{T_{ref}} - \frac{1}{T}\right)\right] \qquad (15)$$

Eg is the bandgap energy of the semiconductor used in the PV cell. IRS is the cell's reverse saturation current at STC which can be expressed as: -

$$I_{Rs} = \frac{I_{sc}}{exp\left(\frac{q.V_{oc}}{N_s.K.n.T}\right)-1} \qquad (16)$$

Voc is the open-circuit voltage of the PV cell when the PV cell's terminal point is open circuit and the output current is zero. Isc is the short circuit current (when the cell terminals are short-circuited) with the maximum value of the current generated by PV Cell and the terminal voltage is zero.
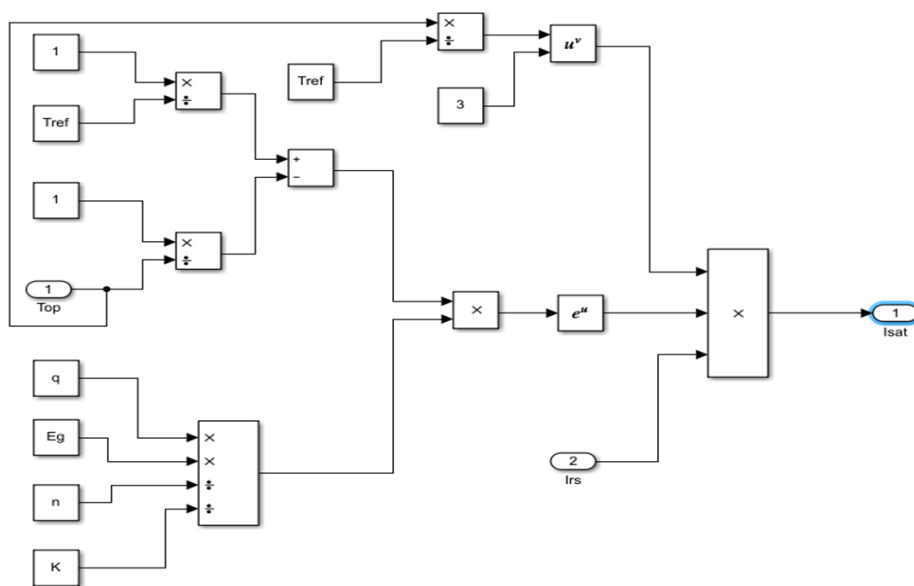Equations 15 and 16 can be expressed in Fig. 15 and Fig. 16 respectively using Matlab-Simulink.

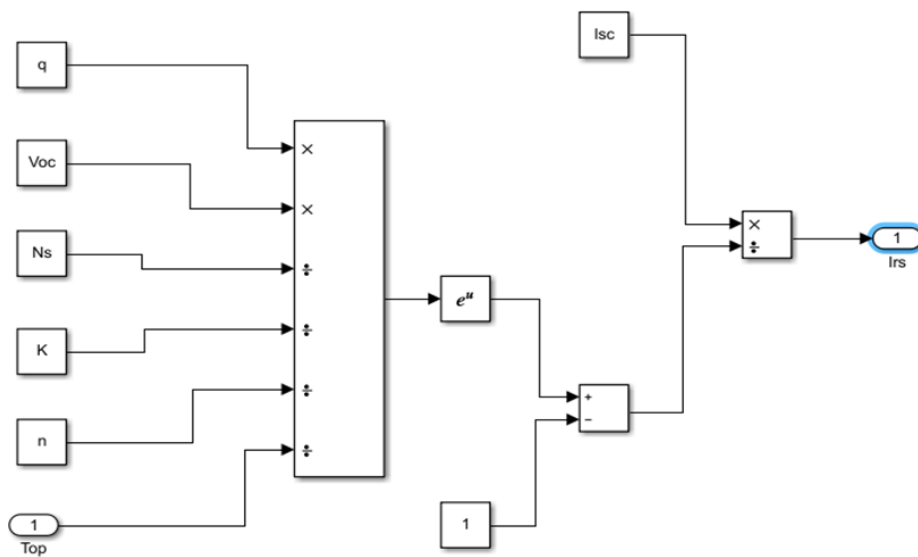**Figure. 15.reverse saturation current of the diode (Isat)**

Figure.16. reverse saturation current of the cell (Irs)

The equations (13) and (14) can be substituted in equation (12) to conclude equation (17) as: -

$$ I = I_{ph} - I_{sat} \left[exp(\frac{V + I.R_S}{n.V_t}) - 1 \right] - \frac{V + I.R_S}{R_{sh}} \qquad (17) $$

The Simulink model of the photovoltaic module is validated with a PV module of SOLIMPEKS PV at STC (1kW/m^2, 25^{0}C) with specifications as shown in Table 3 [29].

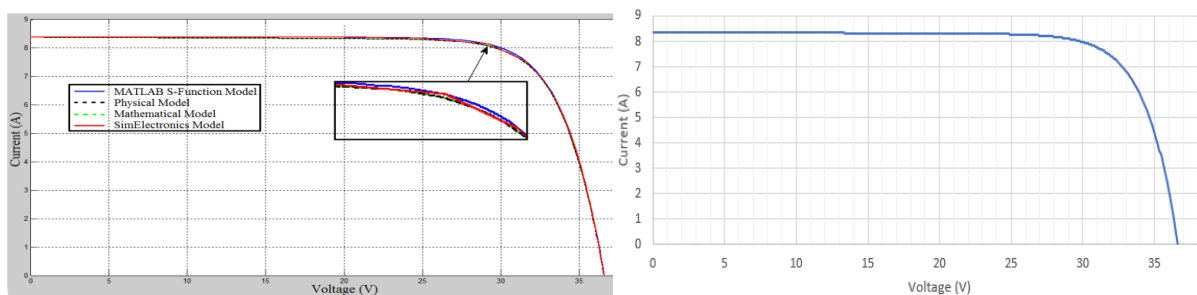| Characteristics of parameters	Specifications
Typical maximum power (Pmp)	240 Watt Voltage
at maximum power (Vm)	30.72 Volt current
at maximum power (Im)	7.81 Amp
Open circuit voltage (Voc)	36.6 Volt
Short circuit current (Isc)	8.36 Amp
No. of cells in Module	60 cells Temp.
coefficient of short circuit current	0.4*10^{-3} A/C^0

Table.3. SOLIMPEKS PV module specifications

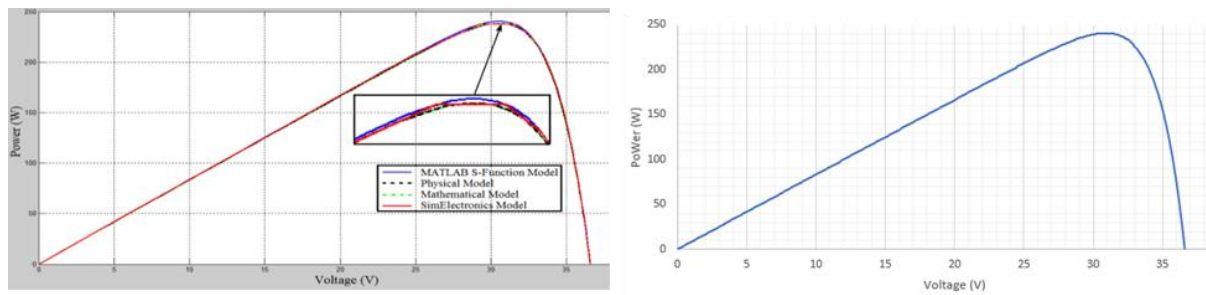**Figure 17: I-V Characteristic Curve Validation**

Figure.18. P-V Characteristic Curve Validation

PHOTOVOLTAIC MODULE SELECTION

In the current market, there are three prevailing technologies concerning photovoltaic panel solar cells [25]: -
- Mono-crystalline or Single-crystalline
- Poly-crystalline
- Thin film

The Mono-crystalline type is selected as it has a bigger efficiency than poly-crystalline and Thin-film type. Therefore, a survey is made for high efficiency and high power for a PV module of mono-crystalline cell type.

The YS510M-96 PV module is selected with maximum power (Pmax) 510 W, voltage at maximum power (Vmpp) 48.5 V, current at maximum power (Impp) 10.51 A, open-circuit voltage (Voc) 59.5 V, short circuit current (Isc) 10.72 A, 96 series cell number is used for a module with efficiency of 19.90 %.

The simulation of the selected PV module is shown in Fig. 19, where the load resistance working as a load on the PV module which is the battery, this load resistance can be controlled using the maximum power point tracking (MPPT) for extracting maximum available power (MPP) from PV cell/module under certain conditions [33].
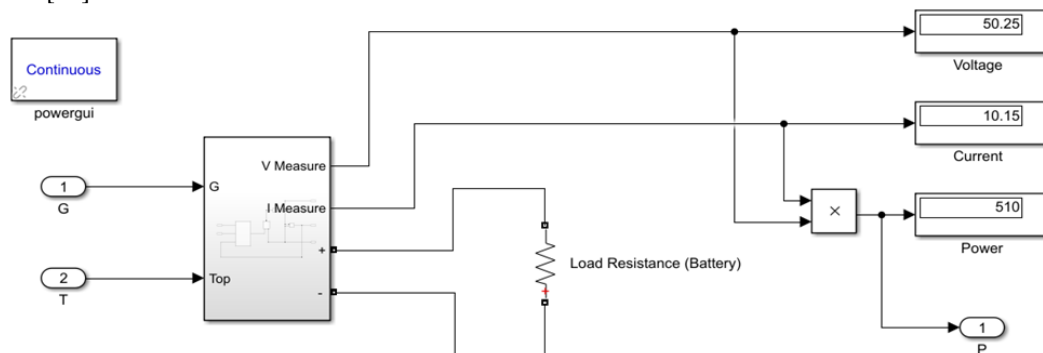

F**igure.19.Simulation model of the selected solar panel module.**

To get more power from the solar panel system, the PV module can be connected in series, parallel, or both to get a PV array. In this study, two PV module is connected in series.

ENERGY CONSUMPTION AND BATTERY SOC (%)

In this study, two types of the road surface are considered (asphalt and sand) each one has a coefficient of rolling resistance (Crr) of 0.029 and 0.05 respectively. Using Simulink manual switches to choose between different tractor's conditions of (grade resistance, road surface type, and drawbar resistance), eight conditions can be obtained from the solar assist plug-in electric tractor as shown in Table 4 to get the energy consumption and SOC at each condition by Matlab Simulink as shown in Fig. 20 and Fig. 21 in results.

Conditions	Grade Resistance		Road Surface Type		Drawbar Resistance	
	Yes	No	Asphalt	Sand	Yes	No
1	No		Asphalt		No	
2	Yes		Asphalt		No	
3	No		Asphalt		Yes	
4	No		Sand		No	
5	Yes		Sand		No	
6	Yes		Asphalt		Yes	
7	No		Sand		Yes	
8	Yes		Sand		Yes	

Table 4. Conditions of the tractor
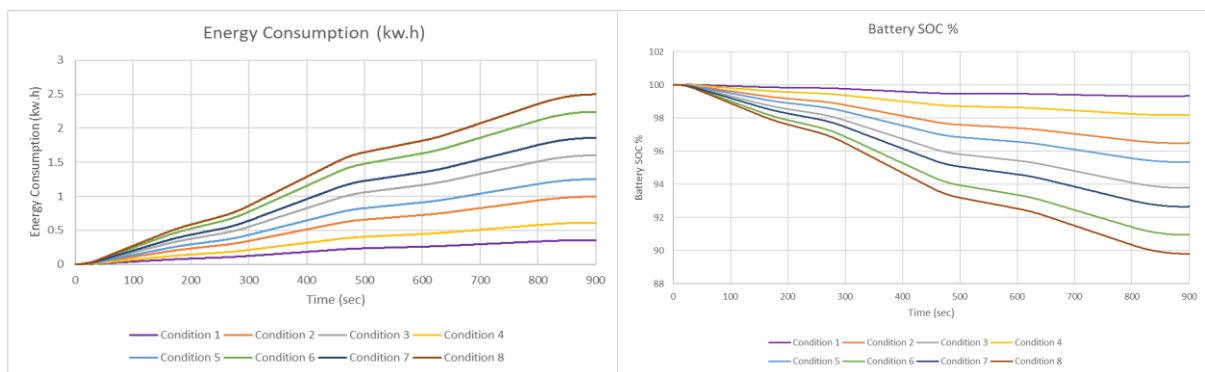
III. RESULTS AND DISCUSSION

Figure.20. Energy Consumption and Battery SOC (%) of the solar assist tractor for each condition

Energy consumption and battery state of charge (%) for the solar assist electric tractor at each condition are obtained in Fig. 20. Condition 1 where there is no road slop or drawbar force with asphalt road type is the lowest energy consumption thus the highest battery state of charge SOC (%) at the end of the drive cycle. While condition 8 where road slop and drawbar force are existing with the soil road surface. this condition has the highest energy consumption with the lowest SOC (%) of the battery.
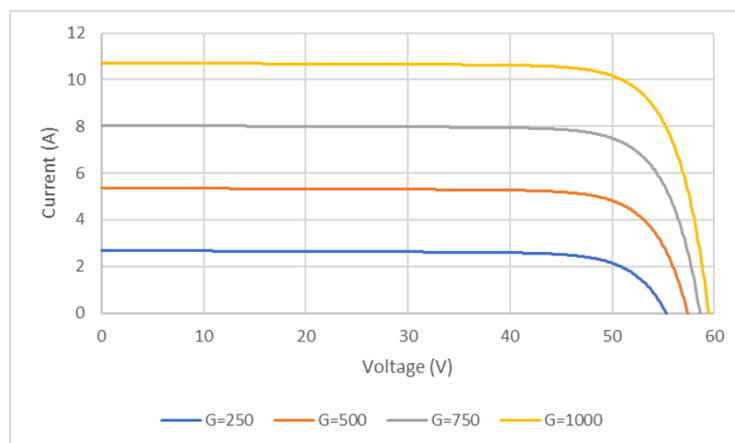

Figure. 21. I–V characteristics, varying irradiance at a constant temperature.

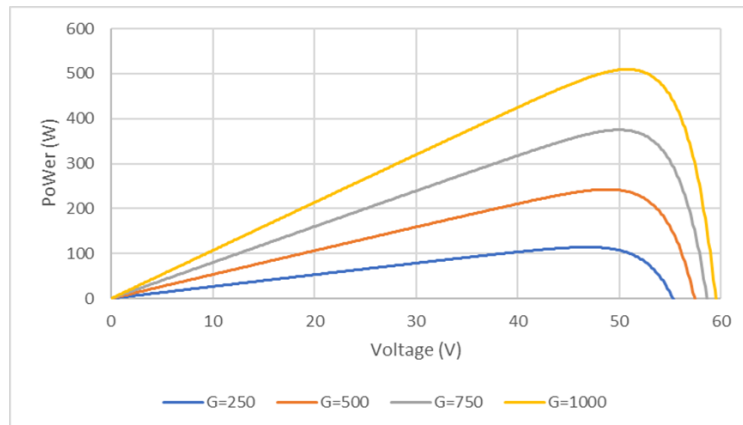Fig. 21 and Fig.22 show the effect of varying irradiance at a constant temperature on PV module behavior.

Figure 22. I–V characteristics, varying irradiance at a constant temperature.

When the irradiance increases, the voltage and current output of the PV module increase. The increasing rate of the current is more than the voltage, where the voltage is less sensitive to the variation of solar insolation as shown in Fig. 21.

Therefore, it is logical the increasing of power in Fig. 22 as irradiance increases due to current increasing.
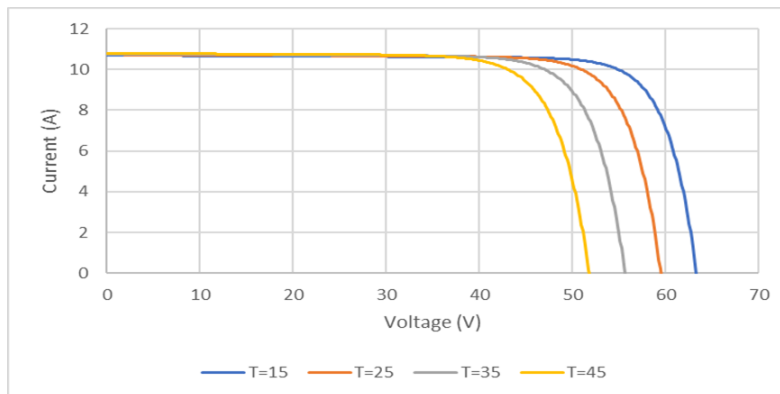

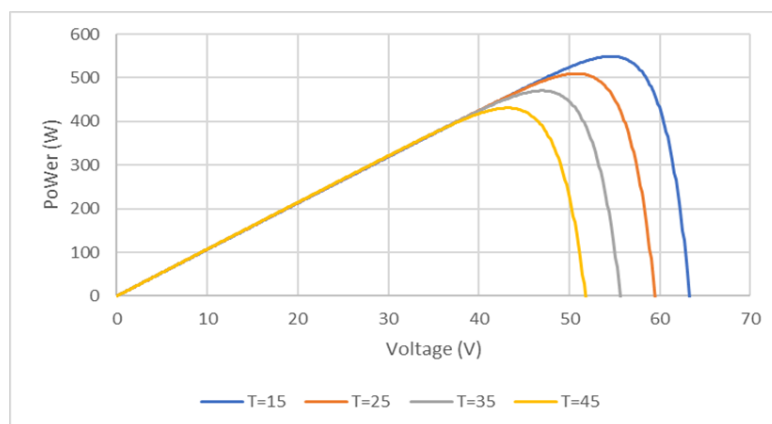**Figure. 23. I–V characteristics, varying temperature at constant irradiance.**

Figure. 24. P–V characteristics, varying temperature at constant irradiance.

In Fig. 23 and Fig. 24, the effect of varying operating temperatures on PV module behavior is obtained. When the temperature increases, the output current increases marginally whereas the voltage decreases drastically. Thus, a decrease in power occurs with operating temperature increases.
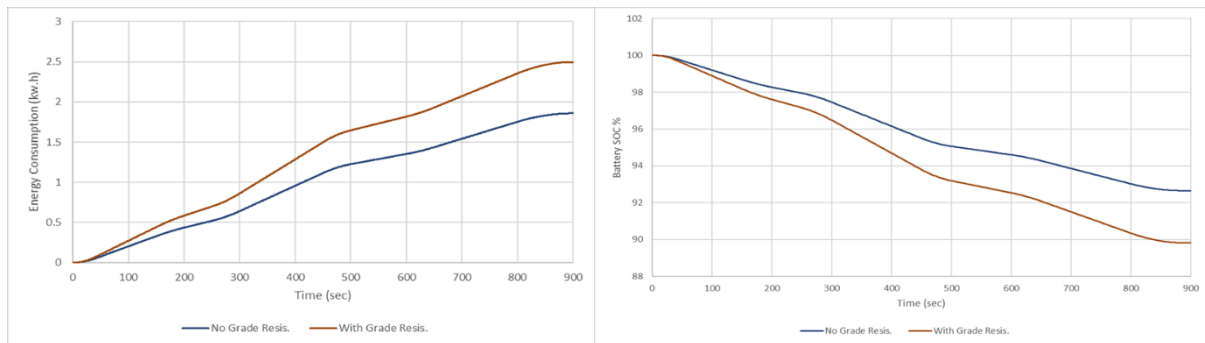

Figure. 25. Effect of grade resistance on energy consumption and battery SOC (%)

Energy consumption increases with existing of the grade resistance, therefore battery SOC decreases with almost 3% less than the condition without road gradient at the end of the drive cycle.
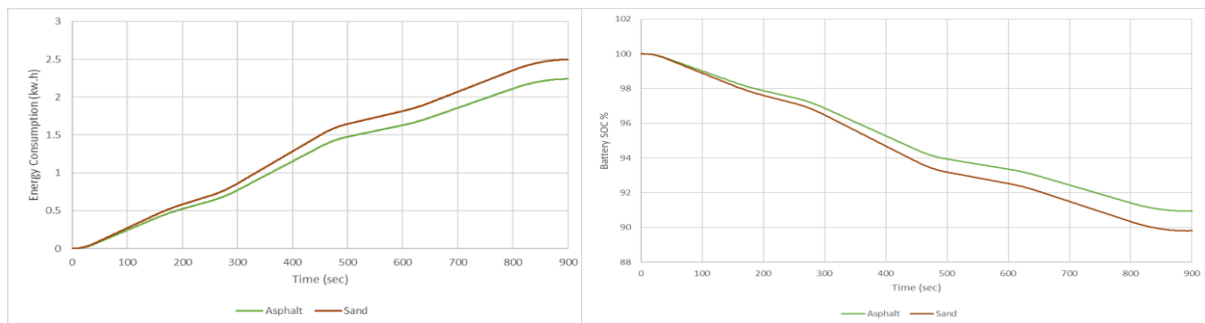

Figure. 26. Effect of road surface type on energy consumption and battery SOC (%)

Energy consumption increases with sand road surface than asphalt because the rolling resistance coefficient of the sand is more than the asphalt. The battery state of charge decreases with sand for around 1.25 % less than asphalt.
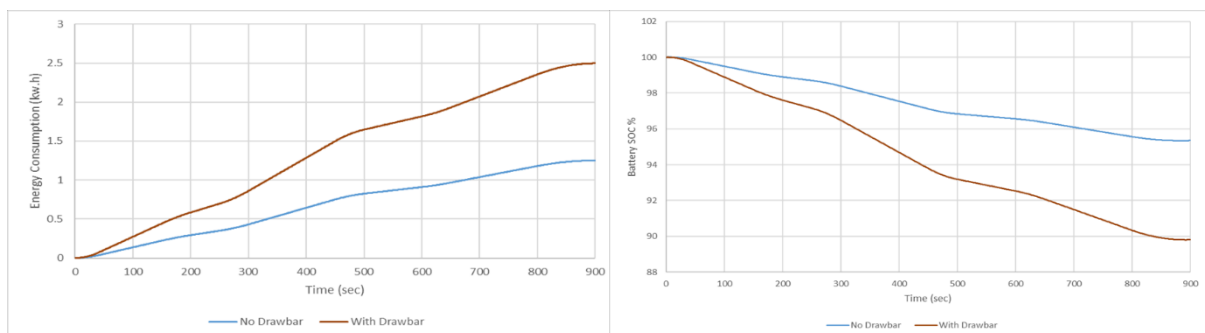

Figure.27. Effect of drawbar force on energy consumption and battery SOC (%)

The drawbar force increases energy consumption as shown in Fig.27 In contrast, the battery state of charge decreases. In this study, the battery SOC (%) decreases with existing of the drawbar force with 5.8 % less than the tractor's condition without drawbar force resistance.

In this study, drawbar resistance was the most influential on increase in energy consumption and thus decreased battery SOC (%), followed by grade resistance then road surface type.
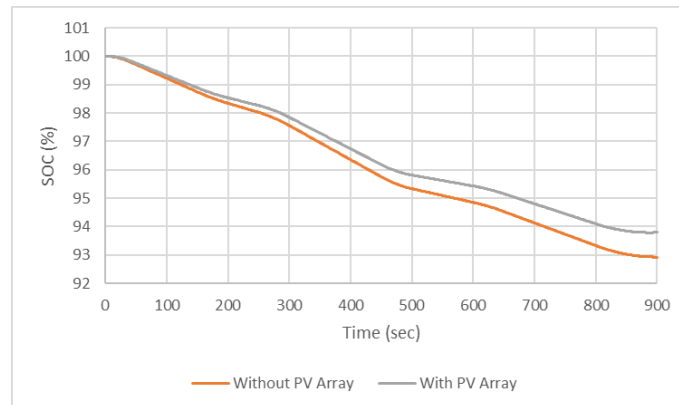

Figure.28. Effect of the PV array on the battery SOC (%)

As Fig.28 shows, the battery state of charge SOC increases with PV array in condition 3 with 0.9 % more than tractor without PV array. The reason for the slight increase in battery SOC is the small value of the PV array energy compared to the battery capacity especially with the drive cycle time of 900 sec. while the PV array can supply the battery with around (817.6 W * 5 hr= 4 kW.hr) for 5 hr that's the average sunrise time in Egypt assuming that operating in the ideal case of STC where G= 1000 W/m^2 and T= 25°C. The percentage of energy provided by the PV array to the energy consumed at each condition is obtained in Table 5.

Condition	Energy Consumed (KW.hr)	Energy provided by PV array compared with consumed (%)
1	0.35	58.4
2	0.99	20.6
3	1.60	12.7
4	0.61	33.4
8	1.25	16.3
6	2.24	9.1
7	1.85	11
8	2.49	8.2

Table 5. Energy provided by PV array as a percentage of the consumed at each condition.

Since the condition 1 is less energy consumption as table 5 shows, then the energy provided from the PV array compared with the consumed will be the highest. And vice versa with condition 8.

IV. CONCLUSION

A solar assist plug-in electric tractor is simulated using the Matlab-Simulink program in this study. Condition 1 is the least energy consumed with the highest SOC (%) while condition 8 is the highest energy consumption with the least battery state of charge. Increased solar radiation positively affects the performance of the solar panel module but the performance of the PV module is negative affected with increased temperature. Battery SOC is decreased by 3% with road slop than without road slop exist. Sand road decreases the SOC by 1.25 % than an asphalt surface type. The battery state of charge is less with 5.8 % with a drawbar than no drawbar. The PV array can provide 4 kW.h daily to charge the battery at ideal operating conditions.

The photovoltaic array can be more effective for the electric tractor with increasing and development of its efficiency, where it needs a large area of PV arrays to get more power due to the low efficiency of the PV cell. More development in battery technology is needed to get higher energy density.

REFERENCES

[1] A. Muniappan, C.T. rajan, G.A. Kumar, X.J. Raj, J. Irene, N. Niranjan, Conversion of Conventional Vehicle into Solar Powered Electric Vehicle - A Realistic Approach, Int. J. Innov. Res. Sci. Eng. Technol. 03 (2014) 16232–16237. https://doi.org/10.15680/ijirset.2014.0309060.

[2] P.D. Kale, N.R. Patel, G.N. Raut, R.B. Lanjewar, Design and implementation of PSoC microcontroller based photovoltaic system, 2014 Int. Conf. Circuits, Power Comput. Technol. ICCPCT 2014. (2014) 1257–1262. https://doi.org/10.1109/ICCPCT.2014.7054966.

[3] S. Kassatly, The Lithium-Ion Battery Industry For Electric Vehicles, (2010).

[4] B. Sri Kaloko, mr.Soebagio, M. Hery Purnomo, Design and Development of Small Electric Vehicle using MATLAB/Simulink, Int. J. Comput. Appl. 24 (2011) 19–23. https://doi.org/10.5120/2960-3940.

[5] A.O. Kıyaklı, H. Solmaz, Modeling of an Electric Vehicle with MATLAB/Simulink, Int. J. Automot. Sci. Technol. (2019) 9–15. https://doi.org/10.30939/ijastech..475477.

[6] D.A.G. Redpath, D. McIlveen-Wright, T. Kattakayam, N.J. Hewitt, J. Karlowski, U. Bardi, Battery powered electric vehicles charged via solar photovoltaic arrays developed for light agricultural duties in remote hilly areas in the Southern Mediterranean region, J. Clean. Prod. 19 (2011) 2034–2048. https://doi.org/10.1016/j.jclepro.2011.07.015.

[7] L. Abdallah, T. El-Shennawy, Reducing carbon dioxide emissions from electricity sector using smart electric grid applications, J. Eng. (United Kingdom). 2013 (2013). https://doi.org/10.1155/2013/845051.

[8] C. Zhang, H. Gao, X. Deng, Z. Lu, Y. Lei, H. Zhou, Design method and theoretical analysis for wheel-hub driving solar tractor, Emirates J. Food Agric. 28 (2016) 903–911. https://doi.org/10.9755/ejfa.2016-05-500.

[9] M.N.A..Mr.Darekar R.D, Mr. Kurhade R.G, Mr. Ponde C.P, SOLAR POWERED VEHICLE, Int. J. Eng. Sci. Manag. Res. (2017) 83–84.

[10] Y. Ueka, J. Yamashita, K. Sato, Y. Doi, Study on the development of the electric tractor-Specifications and traveling and tilling performance of a prototype electric tractor, Eng. Agric. Environ. Food. 6 (2013) 160–164. https://doi.org/10.1016/S1881-8366(13)80003-1.

[11] S.J. Reddy, Estimation of global solar radiation, Sol. Energy. 26 (1981) 279. https://doi.org/10.1016/0038-092X(81)90216-4.

[12] M.N.H. Comsan, Solar Energy Perspectives in Egypt, 4th Environ. Phys. Conf. (2010) 10–14.

[13] Stephen Heckeroth, Electric Tractor, United States Patent No: US 7828099 B2, 2010.

[14] M.A. Elamin, A comparative evaluation of electric- and gasoline- powered garden tractors, Iowa State Univ. Capstones, Theses Diss. (1981).

[15] R.R. Melo, F.L.M. Antunes, H.H. Vogt, D. Albiero, L. Fernando, Conception of an electric propulsion system for a 9 kW electric tractor suitable for family farming, IET Electr. Power Appl. 13 (2019) 12. https://doi.org/10.1049/iet-epa.2019.0353.

[16] H. Mousazadeh, A. Keyhani, A. Javadi, H. Mobli, K. Abrinia, A. Sharifi, Evaluation of alternative battery technologies for a solar assist plug-in hybrid electric tractor, Transp. Res. Part D Transp. Environ. 15 (2010) 507–512. https://doi.org/10.1016/j.trd.2010.05.002.

[17] R.O. Magalhães, M.V. da Assunção, J.P.M. Santos, E.V. da Silva, L. de G. Ferreira Júnior, R.R. Magalhães, D.D. Ferreira, Review on applications of electric vehicles in the countryside, Ciência Rural. 47 (2017). https://doi.org/10.1590/0103-8478cr20161076.

[18] Jonas Engström, Oscar Lagnelöv, An Autonomous Electric Powered Tractor—Simulation of All Operations on a Swedish Dairy Farm, J. Agric. Sci. Technol. A. 8 (2018) 182–187. https://doi.org/10.17265/2161-6256/2018.03.006.

[19] X. Zhang, Design Theory and Performance Analysis of Electric Tractor Drive System, 6 (2017) 235–239.

[20] A. Das, Y. Jain, M.R.B. Agrewale, Y.K. Bhateshvar, K. Vora, Design of a Concept Electric Mini Tractor, 2019 IEEE Transp. Electrif. Conf. ITEC-India 2019. (2019) 10–14. https://doi.org/10.1109/ITEC-India48457.2019.ITECIndia2019-134.

[21] H.I.A.A. Ramy Zakaria Emara, Mohamed A. Eltawil, Said E. AbouZaher, Gamal H. Elsayed, PERFORMANCE OF A PHOTOVOLTAIC SYSTEM TO POWER A DEVELOPED ELECTRIC TRACTOR, in: ROLE Agric. Biol. Eng. Adv. Agric. Sect., 2017.

[22] A.S. H. Mousazadeh, A. Keyhani, A. Javadi, H. Mobli, K. Abrinia, OPTIMAL POWER AND ENERGY MODELING AND RANGE EVALUATION OF A SOLAR ASSIST PLUG-IN HYBRID ELECTRIC TRACTOR (SAPHT), Am. Soc. Agric. Biol. Eng. 53 (2010). https://doi.org/10.13031/2013.32586.

[23] E. Schaltz, Electrical Vehicle Design and Modeling, Electric Vehicles - Modelling and Simulations, 2011. https://doi.org/10.5772/20271.

[24] M.A. KUNT, Advisor Based Modeling of the Effect of Rolling Resistance on Regenerative Braking in All-Electric Passenger Cars, El-Cezeri Fen veMühendislikDerg. 6 (2019). https://doi.org/10.31202/ecjse.603421.

[25] Konstantinos MichailAkritidis, Solar Charged Electric Farming Tractors, Strathclyde Engineering, 2015.

[26] E.M.M. Allam, N.M. Hammad, A.A.A. Saad, S.A. Abouel-seoud, a Small City Series Hybrid Electric Vehicle : Performance Evaluation, EET-2007 Eur. Ele-Drive Conf. (2007).

[27] TM4 SUMO, Direct-drive electric powertrain systems, (2017).

[28] Torque - RPM Curve of the Electric motor, (n.d.). https://www.tm4.com/products/systems/sumo-md/.

[29] N.H.S. Jawad Radhi Mahmood, Four MATLAB-Simulink models of photovoltaic system, Int. J. Energy Environ. 7 (2016) 417–426.

[30] H. Bellia, R. Youcef, M. Fatima, A detailed modeling of photovoltaic module using MATLAB, NRIAG J. Astron. Geophys. 3 (2014) 53–61. https://doi.org/10.1016/j.nrjag.2014.04.001.

[31] H. Yatimi, E. Aroudam, M. Louzazni, Modeling and Simulation of photovoltaic Module using MATLAB/SIMULINK, MATEC Web Conf. 11 (2014) 03018. https://doi.org/10.1051/matecconf/20141103018.

[32] M.T. Scholar, A. Prof, MODELING OF SOLAR PHOTOVOLTAIC MODULE & EFFECT OF INSOLATION VARIATION USING MATLAB / SIMULINK Address for Correspondence, Int. J. Adv. Eng. Technol. IV/III (2013) 5–9.

[33] R. Chandra Meena, S.K. Sharma, Mathematical Modeling of photovoltaic cells Using Matlab/Simulink and MPPT Techniques, Int. J. Adv. Res. Electr. 4 (2015) 7170–7175. https://doi.org/10.15662/ijareeie.2015.0408086.